EnvironmentAsia
The international journal by the Thai Society of Higher Education Institutes on Environment

EnvironmentAsia 12 (Special issue) (2019) 18-27
DOI 10.14456/ea.2019.59
ISSN 1906-1714; ONLINE ISSN: 2586-8861

Transboundary Air Pollution in Relation to Open Burning in Upper Southeast Asia

Souninthone Choommanivong[1], Wan Wiriya[2,3], and Somporn Chantara[2,3*]

[1]*Master's Degree Program in Environmental Science, Environmental Science Research Center, Faculty of Science, Chiang Mai University, Chiang Mai, 50200, Thailand*

[2]*Environmental Science Research center, Faculty of Science,Chiang Mai University, Chiang Mai 50200, Thailand*

[3]*Environmental Chemistry Research Laboratory, Chemistry Department, Environmental Science Program, Faculty of Science,Chiang Mai University, Chiang Mai 50200, Thailand*

*Corresponding author: somporn.chantara@cmu.ac.th

Abstract

This study aims to analyse fire hotspots using two NASA's sensor systems; Moderate Resolution Imaging Spectroradiometer (MODIS), and Visible Infrared Imaging Radiometer Suite (VIIRS) and assess their impacts on air quality. Geographic information system (GIS) was used to create maps of fire hotspots and their density. The Hybrid Single Particle Lagrangian Integrated Trajectory (HYSPLIT) model was used to analyze 24- and 72-hour backward trajectory (BWT) of air mass movement to Chiang Mai city during February-April 2018. Two levels of air mass arriving were set at 10 m and 1,500 m above ground level (AGL). During the study period, directions of air mass movement were mostly from western and south-western of the city. Burned areas obtained from both MODIS and VIIRS systems were significantly different ($p < 0.05$). Correlations between $PM_{2.5}$ concentrations and Burned areas for both 24-and 72-hour BWT obtained from VIIRS were better than those of MODIS at both levels (10 and 1,500 m AGL). Influence of local open burning on air pollution was observed from both systems but VIIRS provided slightly higher correlation with hotspot number than MODIS. Both systems provided similar results for transboundary air pollution (1,500 m AGL).

Keywords: Fire Hotspot, Backward Trajectory, Air pollution, $PM_{2.5}$, Open burning

1. Introduction

Air pollution is a transboundary issue in Southeast Asia (SEA), impacting environment and human health. The major sources of air pollution are open burning including forest fires and agricultural residue burning. Northern Thailand faces with air pollution almost every year during dry season (February to April). Moreover, Chiang Mai Province is located in the basin surrounding by high mountains, which is natural factor promoting pollutant accumulation in the area. Meteorological conditions such as calm wind and high air pressure resulting in low level of mixing height and low vertical air ventilation. Therefore, air pollution is accumulated in this area. Particulate matters (PM) with diameter less than 10 micrometers (PM_{10}) and less than 2.5 micrometers ($PM_{2.5}$) are major concerns due to health impacts. It was reported that PM_{10} correlated with fire hotspot number, but it was inversely correlated with rainfall (Wiriya *et al*., 2013).

Thailand's National Ambient Air Quality Standards (NAAQS) for 24 hours average of PM_{10} and $PM_{2.5}$ concentrations were 120 and 50 μg/m^3, respectively. $PM_{2.5}$ cause both chronic and acute diseases related to respiratory and cardiovascular system due to its interactions with the respiratory tract, lungs, and blood stream (Alias *et al*., 2007; Pochanart, 2012).

The active fire hotspots could be used to represent open biomass burning. Two NASA Earth Observing System (EOS) Moderate Resolution Imaging Spectroradio - meter (MODIS) sensors had observed the earth which could detect fire hotspot in 1 km of resolution (latitude and longitude) by the Terra satellite in the morning orbit and Aqua satellite in the afternoon orbit since they were launched in December 1999 and May 2002 respectively. The NASA/NOAA Visible Infrared Imager Radiometer Suite (VIIRS) sensor was launched in October 2011 on the Suomi National Polar-orbiting Partnership (SNPP) satellite in the afternoon orbit which 375 m of resolution (ESDIS, 2015; Wolfe *et al*, 2012). This study aims to compare $PM_{2.5}$ and number of fire hotspots obtained from both MODIS and VIIRS systems and their relations to air pollution.

2. Materials and Methods

2.1 $PM_{2.5}$ concentration data

Daily $PM_{2.5}$ samples (24 hours) were collected during February to April 2018 at Mae Hia Air Quality Monitoring (MH-AQM) station using a mini-volume air sampler (MiniVol, Airmetrics, USA). Sample number of $PM_{2.5}$ was71 samples.

2.2 Hotspot detection during burning season in upper Southeast Asia (5 counties)

MODIS and VIIRS active fire data during burning season (February – April in 2018) were downloaded from NASA website (https:// earth data.nasa.gov/earth-observation-data/near-real-time/firms/active-fire-data). Number of hotspots obtained from both MODIS and VIIRS systems were compared. Monthly fire hotspot maps during burning season 2018 were constructed. In addition, density maps representing the number of fire hotspots per unit area were analyzed (ESRI, 2018).

2.3 Burned area calculation

Burned area (km^2) was calculated from fire hotspot number multiplying with resolution of the sensor system (1 km × 1 km for MODIS and 0.375 km × 0.375 km for VIIRS).

2.4 Backward Trajectory analysis

Backward trajectories (BWT) of 24- and 72-hours arriving at MH-AQM station (the sampling site) were calculated during sampling period (dry season in 2018) by using the hybrid single particle langrangian integrated trajectory (HYSPLIT-4) model version 4 (Draxler & Hess, 1998). Data from NCEP/NCAR Reanalysis meteorological database; more details about the HYSPLIT model can be found at https:// www. arl.noaa.gov/hysplit/hysplit/ (NOAA Air Resources Laboratory). The arriving time is 02:00 UTC (09:00 LT-local time), at 10 m and 1,500 m above ground level (AGL). The GIS-based software TrajStat was used to create trajectory clustering (Khamkaew *et al*., 2016; Zhao *et al*., 2015).

2.5 Hotspots counting on Backward Trajectory

Buffer zone of diary trajectory lines (±10 km) during sampling period was created by using polyline buffer analysis tool in GIS software. After that, the intersect analysis tool was used to count the number of hotspots (MODIS and VIIRS) in buffer zone along with Trajectory lines.

2.6 Statistical analysis

Pearson's correlation was used to analyze data between $PM_{2.5}$ concentration and hotspots areas within the buffer zone of each trajectory line from both sensor systems (MODIS and VIIRS).

3. Results and Discussion

3.1 $PM_{2.5}$ variation

Figure 1 shows daily $PM_{2.5}$ concentration collected at the sampling site and rain amount during burning season (February-April 2018). Mean $PM_{2.5}$ concentration (n = 71) was 45.48 μg/m^3, while minimum and maximum values were 46.04 and 185.3 μg/m^3, respectively. There was 22 samples (12% of total) with $PM_{2.5}$ concentration higher than the national ambient air standard of Thailand (50 μg/m^3). In addition, $PM_{2.5}$ concentration decreased when rain amount was high.

3.2 Number of fire hotspots and burned areas

Comparison of fire hotspot number detected by MODIS and VIIRS sensor systems using independent sample *t*-test showed significant difference between two systems. During burning season 2018, hotspot number within 5 countries (Myan-mar, Cambodia, Laos, Thailand and Vietnam) obtained from VIIRS was significantly higher ($p<0.01$) than that from MODIS.

Fire hotspots in 5 countries were found in different time periods. Figure 1 shows daily fire hotspot number within 3 months (February-April 2018) detected by MODIS. Percentages of hotspot number found in each country in descending order were Myanmar (39%), Laos (25%), Cambodia (17%), Thailand (12%) and Vietnam (7%), while those detected by VIIRS were Myanmar (43%), Cambodia (18%), Laos (16%), Thailand (16%) and Vietnam (7%). The total fire hotspot counts in this region within 3 months were 101,590 spots from MODIS and 553,321 spots from VIIRS. The number of hotspots detected by VIIRS was about 5 times higher than MODIS.

Furthermore, fire hotspot number was calculated to burned areas. The results showed that burned areas obtained from MODIS and VIIRS were significantly different ($p<0.01$). Table 1 shows the burned areas in upper SEA (5 countries) calculated from MODIS hotspot numbers detected by MODIS and VIIRS. Total burned area obtained from both systems was highest in March, while April was secondary ranked and lowest in February.

Use of fire hotspot numbers and burned areas detected from both systems could provide different result in some cases. MODIS system showed higher numbers of fire hotspot in Laos than in Cambodia, while VIIRS illustrated the opposite results. The reason was because Cambodia had higher hotspot density than Laos. VIIRS is able to detect each hotspot within the cluster resulting in a higher hotspot number. In this case, pattern of hotspots in

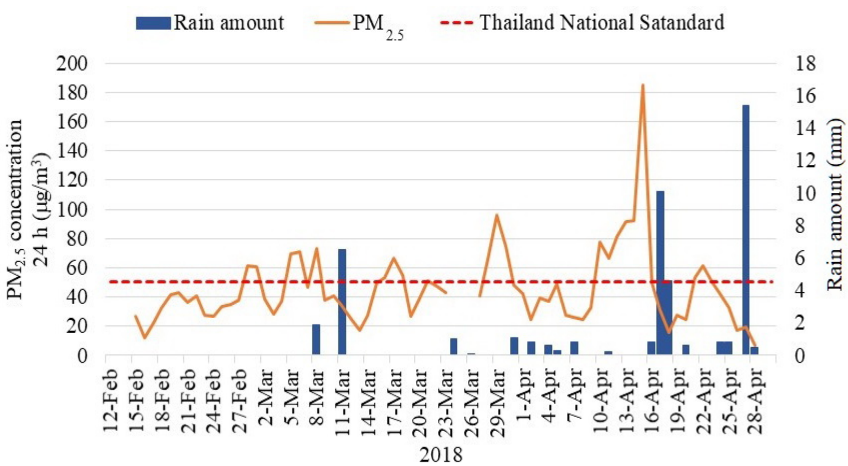

Figure 1. Daily mean $PM_{2.5}$ concentrations and rain amount during burning season (February – April) 2018 at MH-AQM station, Chiang Mai.

Table 1. Burned areas in 5 countries in upper SEA during February–April 2018

Burned area by calculating	Feb		Mar		Apr		Total	
	MODIS	VIIRS	MODIS	VIIRS	MODIS	VIIRS	MODIS	VIIRS
Myanmar	5,276	4,924	21,686	18,712	12,333	9,954	**39,295**	**33,590**
Thailand	3,872	3,102	5,112	5,797	3,138	3,308	**12,122**	**12,207**
Laos	2,371	1,724	8,818	4,120	14,330	6,777	**25,519**	**12,621**
Cambodia	10,814	9,000	4,944	4,062	1,249	1,152	**17,007**	**14,214**
Vietnam	1,626	1,211	3,111	2,052	2,910	1,915	**7,647**	**5,178**
Total	**23,959**	**19,962**	**43,671**	**34,742**	**33,960**	**23,107**	**101,590**	**77,811**

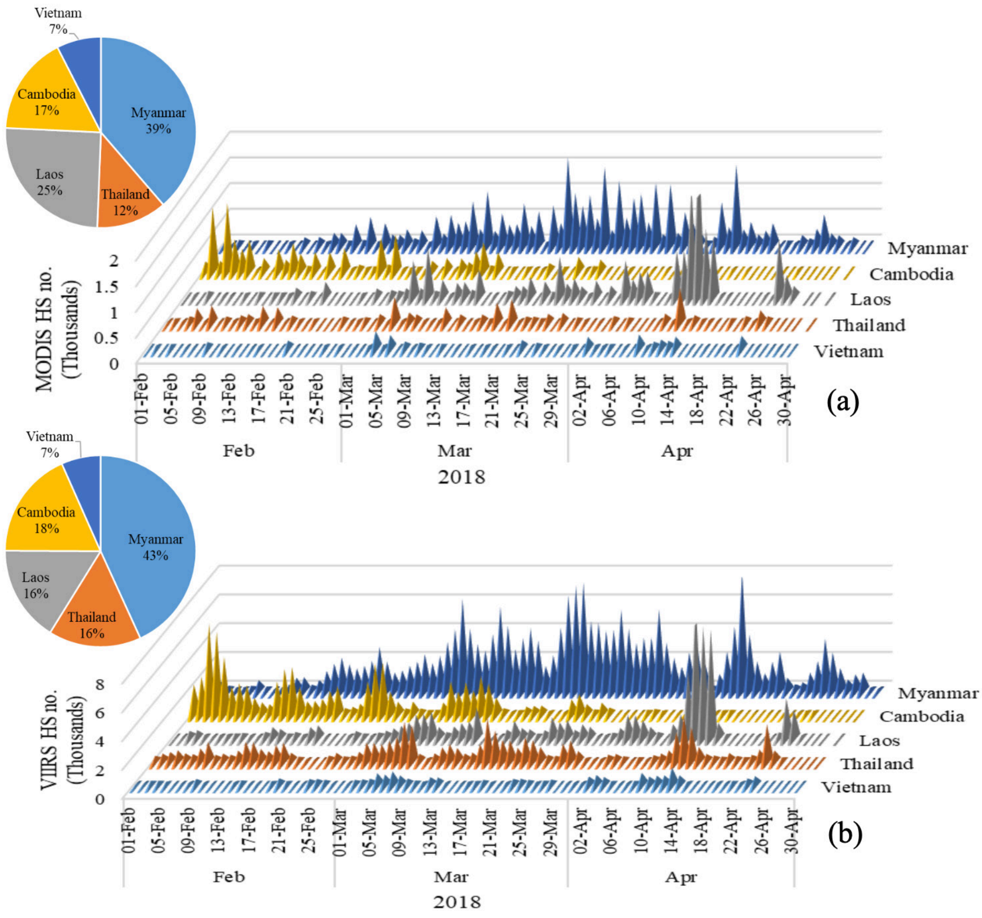

Figure 2. Number of fire hotspots in 5 countries during burning season (February – April) 2018 detected by (a) MODIS and (b) VIIRS sensor systems

Laos had higher distribution than that found in Cambodia, and thus MODIS recognized a higher number of hotspots.

Figure 2 shows variation and percent contribution of fire hotspot occurrence in each country. Fire hotspots were extensive in Cambodia from February until middle of March. In general number of hotspots was very high in March, particularly in Myanmar, Laos and some part of Thailand. Hotspot number in

April was highest in Laos, while it reduced in other areas.

In total, the highest hotspot number from both systems was found in Myanmar (39-43%).

3.3 Distribution of fire hotspot

Monthly distribution of fire hotspots obtained from MODIS and VIIRS systems are shown in Figure 3. These showed that fire hotspot detected by MODIS covered less area than that detected by VIIRS. VIIRS system could detect finer fire hotspots than MODIS system, because VIIRS resolution is 375 m x 375 m, which is approximately 7 times finer than MODIS (1 km × 1 km) (ESDIS, 2015; Wolfe *et al*., 2012). Therefore, MODIS sensor system could detect fire hotspots number less than VIIRS sensor system.

3.4 Density of fire hotspots

The density of fire hotspots in February, March and April 2018 are shown in Figure 4. The densities of fire hotspots detected from both MODIS and VIIRS sensors were similar. In February, the highest density was located in Cambodia. In March, hotspots were shifted to

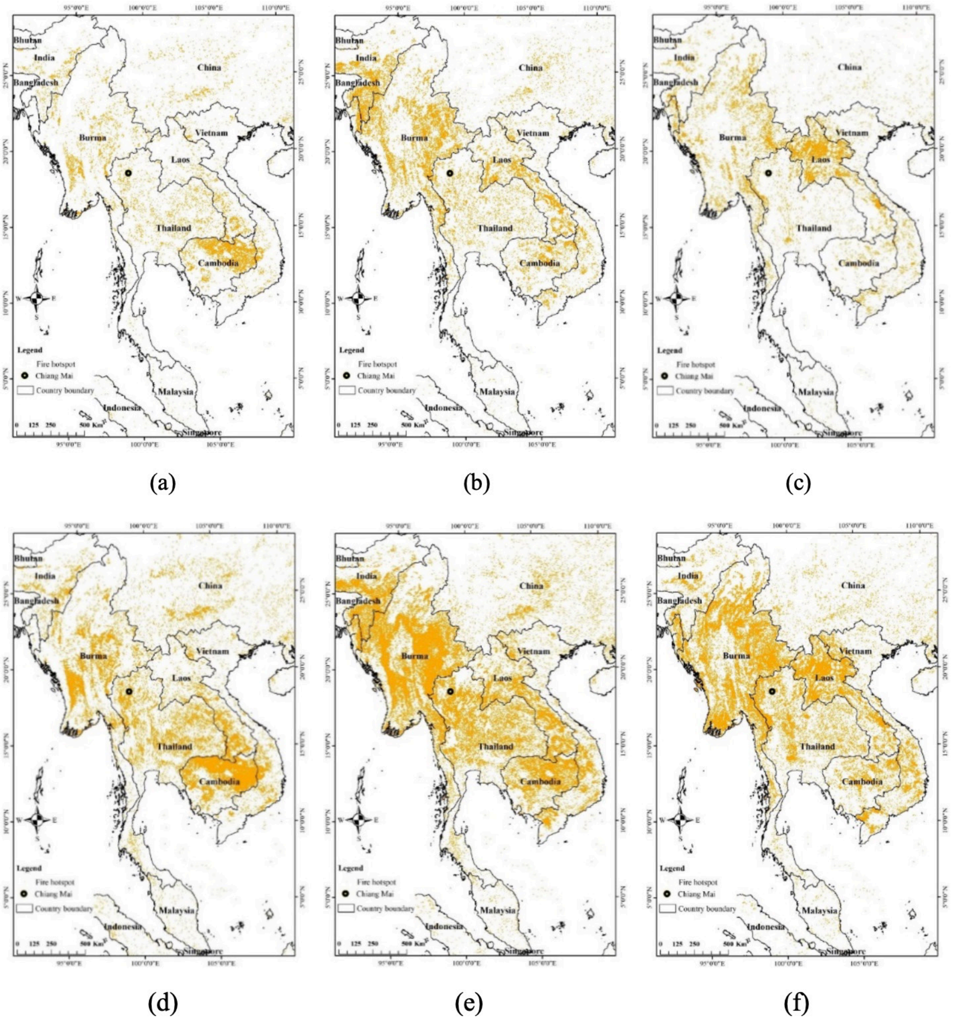

Figure 3. Monthly distribution of fire hotspots obtained from MODIS in February (a), March (b) and April (c), and from VIIRS in February (d), March (e) and April (f)

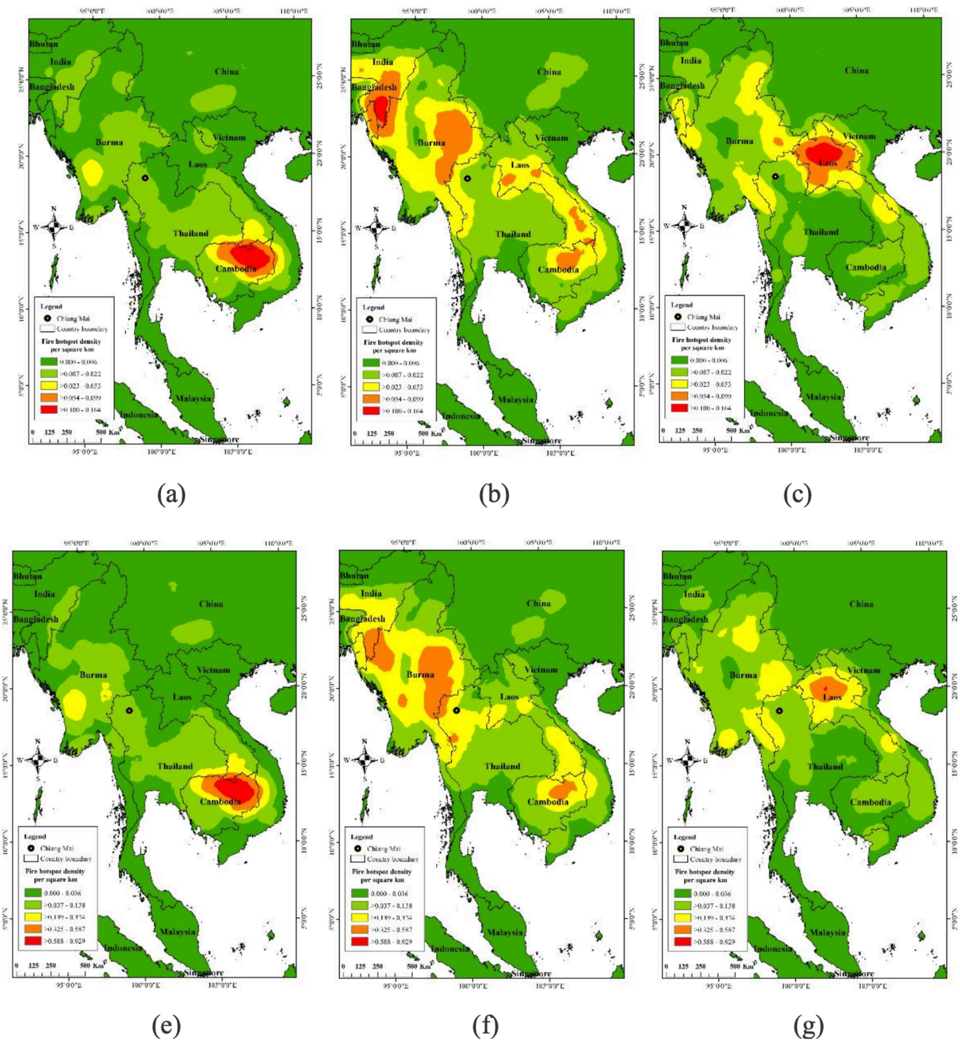

Figure 4. Monthly density of fire hotspots obtained from MODIS in (a) February, (b) March and (c) April and VIIRS in (d) February, (e) March and (f) April

the north (Myanmar and Laos). In April, the highest density was found in Northern Laos. It can be concluded that both sensor systems can be used for construction of fire hotspot density maps with similar precision.

3.5 Air mass movement to Chiang Mai city

Trajectory analysis of 24- and 72-hours BWT was used to calculate air mass movement to Chiang Mai city during open burning season in 2018. Figure 5 shows BWT at 1,500 m AGL arriving, which represent long-range transport. The average length of 24-hour BWT was 318 ±106 km, while that for 72-hour BWT was 1,124 ± 649 km. BWT clustering for both 24- and 72-hour showed major directions of air movement, which were from south, southwest and west directions of Chiang Mai city.

Figure 6 shows BWT at 10 m AGL arriving, which is represented local air mass movement. The average length of 24-hour BWT was 145 ± 79 km, while that for 72-hour BWT was 545 ± 356 km. BWT clustering of both 24- and 72-hours showed main directions of air movement from south, southwest and northeast directions of the city.

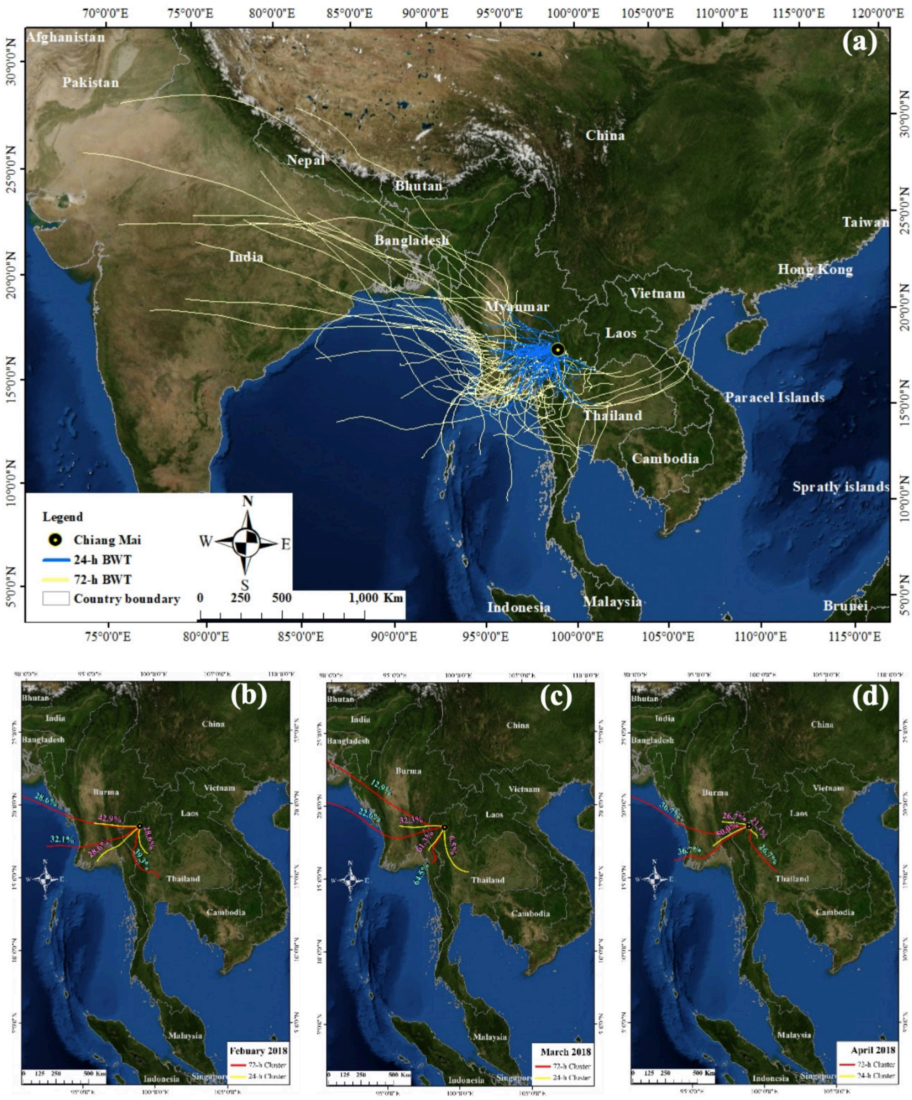

Figure 5. 24- and 72-hours BWTs of air mass movement arriving Chiang Mai city at 1,500 m AGL: (a) during open burning season (February-April 2018). BWT clustering: (b) February, (c) March and (d) April 2018

The direction of BWT clustering is affected from topography i.e. high mountain on the west, therefore, BWT clustering at 10 m AGL could not flow over high mountain. It can be assumed that BWT clustering at 10 m AGL could be obstructed by high mountains.

3.6 Air pollution and burned area correlation

Pearson correlations were used to perform correlations between air pollution ($PM_{2.5}$ concentration) and burn area (Table 2). It was found that VIIRS system provided significant correlation between $PM_{2.5}$ and burned area for all variables (time period of BWT and height of air mass arriving). MODIS system provided significant correlations between $PM_{2.5}$ and burned area for only two variables, which were 24-hour BWT at 10 m AGL and 72-hour BWT at 1,500 m AGL of air mass movement. Thus, application of both VIIRS and MODIS systems for the 24-hour BWT at 10 m AGL was suitable to represent local pollution, while 72-h BWT at both arriving levels can be used to predict transboundary air pollution. It was found that Pearson correlation values of VIIRS system were higher than those of MODIS system, however most of them had low values. The major reason might be due to La Niña effect in this year (2018) resulting in higher amount of rain, which had influence on air pollution (Punsompong & Chantara, 2018; WMO, 2018).

4. Conclusions

VIIRS system obviously provides higher number of active fire hotspots than MODIS, due to finer resolution. However, MODIS can cover larger burned area than VIIRS, but both

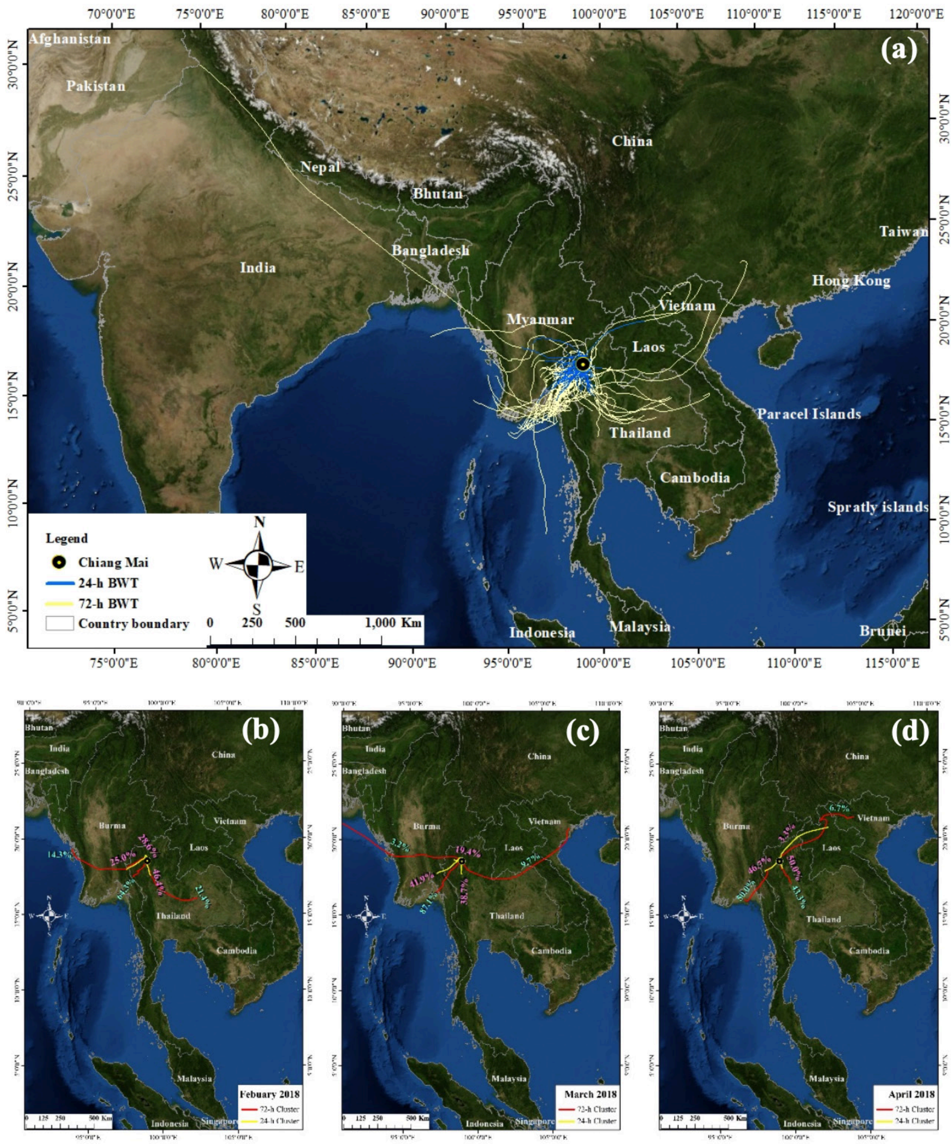

Figure 6. 24- and 72-hours BWTs of air mass movement arriving Chiang Mai city at 10 m AGL: (a) during open burning season (February-April 2018). BWT clustering: (b) February, (c) March and (d) April 2018

Table 2. Pearson correlations between $PM_{2.5}$ and both VIIRS and MODIS burned areas on 24- and 72-day BWT with both 1,500 m and 10 m AGL arriving

Sensor system	24-hour BWT		72-hour BWT	
	10 m AGL	1,500 m AGL	10 m AGL	1,500 m AGL
VIIRS	**.417****	**.261***	**.262***	**.247***
MODIS	**.251***	.210	.144	**.251***

*. Correlation is significant at the 0.05 level (2-tailed).
**. Correlation is significant at the 0.01 level (2-tailed).

systems can be used to demonstrate temporal shifting of burning activity.

Influence of open burning on air quality was also studied by performing BWT of the receptor (Chiang Mai city) at different times and levels of air mass arrival. It was found that the main direction of air mass movement to Chiang Mai city was from the southwest, while some of them were from the west and the south. Air mass movement at ground level (24-hour BWT at 10 m AGL) is suitable to represent local pollution and 72-h BWT at both arriving levels can be used to predict transboundary air pollution. The correlations of the fire area and $PM_{2.5}$ in this year were low due to La Niña effect. However, significant correlations still can be found between $PM_{2.5}$ concentration and burned area.

Acknowledgements

Scholarship from Thailand International Cooperation Agency (TICA) to Mr. Souninthone Choommanivong, master's degree student at Chiang Mai University, is gratefully acknowledged.

References

Alias M., Hamzah Z., & Kenn L. S. PM_{10} and Total Suspended Particulates (TSP) Measurements in Various Power Stations. The Malaysian Journal of Analytical Sciences. 2007; 11(1): 255–261.

Draxler R. R., & Hess G. D. An Overview of the HYSPLIT _ 4 Modelling System for Trajectories , Dispersion, and Deposition. 47 (June 1997). 1998; 295–308.

ESDIS. (2015). Fire Information for Resource Management System (FIRMS). NASA's Goddard Space Flight Center/Earth Science Data and Information System (ESDIS).

ESRI. (2018). Point Density. Retrieved November 21, 2018. [Available from: http://pro.arcgis.com/en/pro-app/ tool-reference/spatial-analyst/ point-density. htm].

Khamkaew C., Chantara S., Janta R., Pani S. K., Prapamontol T., Kawichai S., Lin N. H. . Investigation of biomass burning chemical components over Northern Southeast Asia during 7-SEAS/BASELInE 2014 campaign. Aerosol Air Qual. Res. 2016: 16(11); 2655–2670.

Pochanart P. Air Pollution and Long-range Transport in Asia: (1) East Asia. NIDA Journal of Environmental Management. 1012: 8(1); 57–77.

Punsompong P., & Chantara S. Identification of potential sources of PM_{10} pollution from biomass burning in northern Thailand using statistical analysis of trajectories. Atmospheric Pollution Research. 2018: 9(6); 1038–1051.

Wiriya W., Prapamontol T., & Chantara S. PM_{10}-bound polycyclic aromatic hydrocarbons in Chiang Mai (Thailand): Seasonal variations, source identification, health risk assessment and their relationship to air-mass movement. Atmospheric Research. 2013: 124; 109–122.

WMO. (2018). El Niño _ La Niña Update - June 2018 _ World Meteorological Organization. [Available from: https:// public.wmo. int/en/media/news /el-niño-la-niña-update-june-2018].

Wolfe R. E., Nishihama M., Lin G., Tewari K. P., & Montano E. MODIS and VIIRS geometric performance comparison.

International Geoscience and Remote Sensing Symposium (IGARSS), 2012 IEEE Inter-national. 2012: 5017–5020.

Zhao M., Huang Z., Qiao T., Zhang Y., Xiu G., & Yu J. Chemical characterization, the transport pathways and potential sources of $PM_{2.5}$ in Shanghai: Seasonal variations. Atmospheric Research. 2015: 158–159; 66–78.